The structural connectome constrains fast brain dynamics

Sorrentino P[1,2], Seguin C[3], Rucco R[4,5], Liparoti M[4,5], Troisi Lopez E[4,5], Bonavita S[6], Quarantelli M[7], Sorrentino G[4,5], JirsaV[1*]& Zalesky A[3*]

* Co-senior authors

1. **Institut de Neurosciences des Systèmes, Aix-Marseille University, Marseille, France**
2. **Institute of Applied Sciences and Intelligent Systems, National Research Council, Pozzuoli, Italy**
3. **University of Melbourne, Melbourne, Australia**
4. **Department of Motor Sciences and Wellness, Parthenope University of Naples, Naples, Italy**
5. **Institute for Diagnosis and Cure Hermitage Capodimonte, Naples, Italy**
6. **University of Campania Luigi Vanvitelli, Caserta, Italy**
7. **Biostructure and Bioimaging Institute, National Research Council, Naples, Italy**

Abstract

The activity of the brain during rest displays complex, rapidly evolving patterns in space and time. Structural connections comprising the human connectome are likely to impose constraints on the evolution of this activity. Here, we use magnetoencephalography (MEG) to quantify the extent to which fast neural dynamics in the human brain are constrained by structural connections inferred from diffusion MRI tractography. We characterize the spatio-temporal unfolding of whole-brain activity at millisecond scale from source-reconstructed MEG data, estimating the probability that any two brain regions will activate at consecutive time epochs. We then test whether these probabilities associate with structural connectivity strength. We find that the structural connectome strongly shapes the fast spreading of neuronal avalanches. This finding opens new avenues to study the relationship between brain structure and neural dynamics.

Keywords: brain dynamics, brain networks, magnetoencephalography, neuronal avalanches, structural connectome

Introduction

The structural scaffolding of the human connectome[1] constrains the unfolding of large-scale coordinated neural activity towards a restricted *functional repertoire*[2]. While functional magnetic resonance imaging (fMRI) can elucidate this phenomenon at relatively slow timescales[3–5], brain activity shows rich dynamic behaviour evolving at multiple timescales, with faster activity nested within slower ones. Here, we exploit the high temporal resolution of resting-state magnetoencephalography (MEG) data to study the spread of neuronal avalanches in healthy adults, aiming to establish whether the structural connectome constrains the spread of avalanches among regions[6,7]. We find that spread is significantly more likely between pairs of grey matter regions that are structurally connected, as inferred from diffusion MRI tractography. This result provides cross-modal empirical evidence suggesting that connectome topology constrains fast-scale transmission of neural information, linking brain structure to brain dynamics.

Results

Structural connectomes were mapped for 58 healthy adults (32 males / 26 females, mean age ± SD was 30.72 ± 11.58) using diffusion MRI tractography and regions comprising the Automated Anatomical Labeling (AAL) and the Desikan-Killiany-Tourville (DKT) atlases. Interregional streamline counts derived from whole-brain deterministic tractography quantified the strength of structural connectivity between pairs of regions (see SI extended methods). Group-level connectomes were computed by averaging connectivity matrices across participants.

MEG signals were pre-processed and source reconstructed for both the AAL and DKT atlases. Each source reconstructed signal was z-scored and binarized such that, at any time point, a z-score exceeding a given threshold was set to 1 (active); all other timepoints were set to 0 (inactive). An avalanche was defined as starting when any region exceeded this threshold, and finished when no region was active. An avalanche-specific transition matrix (TM) was calculated, where element (i, j) represented the probability that region j was active at time $t+1$, given that region i was active at time t. The TMs were averaged per participant, and then per group, and finally symmetrized.

We found striking evidence of an association between avalanche transition probabilities and structural connectivity strengths (Fig. 2), suggesting that regional propagation of fast-scale neural avalanches is partly shaped by the axonal fibers forming the structural connectome. The association was evident for different activation thresholds and both the AAL and DKT connectomes (AAL atlas: for threshold z=2.5, r=0.38; for threshold z=3.0, r=0.37; for threshold z=3.2, r=0.34; DKT atlas: for threshold z=2.5, r=0.32; for threshold z=3.0, r=0.31; for threshold z=3.2, r=0.30; in all

cases, $p < 0.0001$), as well as for individual- and group-level connectomes, although associations were stronger for group-level analyses (see Fig. 2, panel A).

Next, we sought to validate the findings using null transition matrices computed after randomizing the times of each avalanche while keeping the spatial structure unchanged (see SI extended methods), yielding transitions consistent with the null hypothesis that the temporal unfolding of activity is unrelated to the structural topology. Null transition matrices resulted in markedly weaker associations with structural connectivity (AAL atlas, z-score=3: mean $r = 0.25$, observed $r = 0.38$, $p<0.001$). This suggests that the empirical organization of the connectome significantly shapes the temporally resolved propagation of neural activity. We replicated these findings for a group-level connectome derived using high-quality data from 200 healthy adults in the Human Connectome Project ($r=0.11$, $p<0.001$, z-score=3; Methods). This indicates that our results are robust to variations in connectome mapping methods and remain significant even when avalanches and structural networks are computed on sets of different subjects (albeit with weaker strength, as compared to the native tractographies).

Discussion

Our results indicate that large-scale structural projections shape the spatio-temporal unfolding of functional interactions among distant brain regions, likely contributing to coherent neural dynamics. The current findings provide new insight into the propagation of fast-evolving brain activity across structural brain networks. Our results confirm that structural connections bias the propagation of activations to regional loci that are interconnected by axonal fibres bundles and, hence, constrain the exploration of the brain's state-space.. Previous evidence shows that correlated fluctuations in the BOLD signal partly relate to structure[3,8,9]. However, at higher frequencies, complex patterns appear nested in slow activity[10]. Using MEG data, and showing that reconfiguration of activations is constrained by the brain structural substrate, we suggest that the known correlation between the long-term average resting-state functional magnetic resonance imaging (rsfMRI) connectivity and structure can be understood as the structure influencing dynamic reconfigurations, and thus carrying cognitive and, likely, behavioural meaning[11]. Finally, our results explain how the large-scale activity unfolding in time might lead to the previous observation that average rsfMRI connectivity has topological features that mirror those of the structural connectome[12]. The neural avalanche framework opens up new opportunities to investigate polysynaptic models of network communication, which aim to describe patterns of signalling between anatomically unconnected regions[13,14]. Therefore, our work provides a foundational step towards elucidating the mechanisms governing communication in the human connectome. In turn, this can be exploited to predict the

effects of structural lesions on behaviour and/or clinical phenotypes, under the above-mentioned hypothesis that structure influences behavioural outcomes by constraining global dynamics. In conclusion, using the neuronal avalanches as a paradigm applied to MEG data, we provide a framework to link dynamical brain connectivity to the structural connectome.

Methods

The data were acquired using a MEG system equipped by 154 magnetometers SQUID (Superconducting Quantum Interference Device). The MEG registration is divided in two eyes-closed segments of 3:30 minutes. To identify the position of the head, four anatomical points (nasion, right and left pre-auricular points and vertex of the head) and four position coils were digitized. Electrocardiogram (ECG) and electro-oculogram (EOG) signals were also recorded during the acquisition. The MEG signals, after an anti-aliasing filter, were acquired at 1024 Hz, then a fourth order Butterworth IIR band-pass filter in the 0.5-48 Hz band was applied. To remove environmental noise, measured by reference magnetometers, we used Principal Component Analysis, while we adopted Independent Component Analysis to clean the data from physiological artifacts, such as eye blinking (if present) and heart activity (generally one component). Noisy channels were identified and removed manually by an expert rater. The time series of neuronal activity were reconstructed based on the Automated Anatomical Labeling (AAL) and the Desikan-Killiany-Tourreville (DKT) atlases. To do this, we used the Linearly Constrained Minimum Variance (LCMV) beamformer algorithm based on the native MRIs. Finally, we excluded the ROIs corresponding to the cerebellum because of their low reliability in MEG. However, when these regions were included the results were confirmed. All the preprocessing steps and the source reconstruction were made using the Fieldtrip toolbox. Each source reconstructed signal was binned (such as to obtain a branching ratio ~=1, see SI) and then z-scored and binarized, such that, at any time bin, a z-score exceeding 3 was set to 1 (active); all other time bins were set to 0 (inactive). See supplementary materials for further details. Alternative z-score thresholds (i.e. 2.5 and 3.5) were tested. An avalanche was defined as starting when any region is above threshold, and finishing when no region is active, as in[15]. Avalanches shorter than 10 time bins were excluded in the reported results. However, the analyses were repeated including only avalanches longer than 30 time bins, to focus on rare events that are highly unlikely to be noise, and including all avalanches, and the results were unchanged. An avalanche-specific transition matrix (TM) was defined with rows and columns as regions, while entries as the probability that region j is active at time $t+1$,

given that region *i* has been active at time *t*. The avalanche-specific TMs were averaged per subject, and then per group.

A subject-specific connectome was obtained using diffusion MRI data acquired on the same MRI scanner for all subjects (1.5 Tesla, Signa, GE Healthcare). DTI preprocessing was carried out using the software modules provided in the FMRIB Software Library (FSL, http://fsl.fmrib.ox.ac.uk/fsl). All DTI datasets were corrected for head movements and eddy currents distortions using the "eddy_correct" routine, rotating diffusion sensitizing gradient directions accordingly, and a brain mask was obtained from the B0 images using the Brain Extraction Tool routine. A diffusion-tensor model was fitted at each voxel, and fiber tracks were generated over the whole brain by deterministic tractography using Diffusion Toolkit (FACT propagation algorithm, angle threshold 45°, spline-filtered, masking by the fractional anisotropy (FA) maps thresholded at 0.2). For tractographic analysis, the regions of interest (ROIs) of the AAL atlas and of a MNI space-defined volumetric version of the Desikan-Killiany-Tourville (DKT) ROI atlas were used masked by the GM tissue probability map available in SPM (thresholded at 0.2). To this end, for each patient, FA volumes were normalized to the MNI space using the FA template provided by FSL, using the spatial normalization routine available in SPM12, and the resulting normalization matrices were inverted and applied to the ROIs, to apply them onto each patient's study. The quality of the normalization was assessed visually. From each subject's whole brain tractography and corresponding GM ROI set, the number of streamlines connecting each couple of GM ROIs and the corresponding mean tract length was calculated using an in-house software written in Interactive Data Language (IDL, Harris Geospatial Solutions, Inc., Broomfield, CO, USA). MEG pre-processing and source reconstruction were performed as in[15]. Results were replicated using both the AAL and the DKT atlases. Furthermore, the results were replicated using a group-level connectome constructed from high-quality diffusion MRI data for 200 healthy adults in the Human Connectome Project. Structural connectivity was derived using the AAL atlas and an independent connectome mapping pipeline (see SI). Each symmetrized subject-specific transition matrix was related to the subject-specific DTI using Spearman's correlation. Then, the subject-specific transition matrices were averaged, as well as the related subject-specific structural connectomes. Then, the lower triangular symmetrized averaged transition matrix was related to the lower triangular averaged structural connectome, using Spearman's correlation. The statistical validation was done obtaining surrogate avalanches by randomizing the observed avalanches across time (without changing the order of the avalanches at each timestep) a thousand times. At each iteration, the transition matrix was computed, and related by Spearman's correlation to the structural matrix, thereby building a null distribution of the correlations.

Bibliography

1. Sporns, O., Tononi, G. & Kötter, R. The Human Connectome: A Structural Description of the Human Brain. *PLoS Comput. Biol.* **1**, e42 (2005).
2. Deco, G., Jirsa, V. K. & McIntosh, A. R. Emerging concepts for the dynamical organization of resting-state activity in the brain. *Nature Reviews Neuroscience* vol. 12 43–56 (2011).
3. Honey, C. J., Kötter, R., Breakspear, M. & Sporns, O. Network structure of cerebral cortex shapes functional connectivity on multiple time scales. *Proc. Natl. Acad. Sci. U. S. A.* **104**, 10240–5 (2007).
4. Goni, J. *et al.* Resting-brain functional connectivity predicted by analytic measures of network communication. *Proc. Natl. Acad. Sci. U. S. A.* **111**, 833–838 (2014).
5. Zalesky, A., Fornito, A., Cocchi, L., Gollo, L. L. & Breakspear, M. Time-resolved resting-state brain networks. *Proc. Natl. Acad. Sci. U. S. A.* **111**, 10341–6 (2014).
6. Beggs, J. M. & Plenz, D. Neuronal Avalanches Are Diverse and Precise Activity Patterns That Are Stable for Many Hours in Cortical Slice Cultures. *J. Neurosci.* **24**, 5216–5229 (2004).
7. Shriki, O. *et al.* Neuronal avalanches in the resting MEG of the human brain. *J. Neurosci.* **33**, 7079–7090 (2013).
8. Honey, C. J., Thivierge, J. P. & Sporns, O. Can structure predict function in the human brain? *NeuroImage* vol. 52 766–776 (2010).
9. Honey, C. J. *et al.* Predicting human resting-state functional connectivity from structural connectivity. *Proc. Natl. Acad. Sci. U. S. A.* **106**, 2035–2040 (2009).
10. Saggio, M. L., Spiegler, A., Bernard, C. & Jirsa, V. K. Fast–Slow Bursters in the Unfolding of a High Codimension Singularity and the Ultra-slow Transitions of Classes. *J. Math. Neurosci.* **7**, 1–47 (2017).
11. Mcintosh, A. & Jirsa, V. The hidden repertoire of brain dynamics and dysfunction. *Netw. Neurosci.* **3**, (2019).
12. Bullmore, E. & Sporns, O. Complex brain networks: graph theoretical analysis of structural and functional systems. *Nat. Rev. Neurosci.* **10**, 186–198 (2009).
13. Seguin, C., Van Den Heuvel, M. P. & Zalesky, A. Navigation of brain networks. *Proc. Natl. Acad. Sci. U. S. A.* **115**, 6297–6302 (2018).
14. Seguin, C., Razi, A. & Zalesky, A. Inferring neural signalling directionality from undirected structural connectomes. *Nat. Commun.* **10**, 1–13 (2019).
15. Sorrentino, P. *et al.* Extensive functional repertoire underpins complex behaviours: insights from Parkinson's disease. *bioRxiv* 823849 (2019) doi:10.1101/823849.

Figure 1.

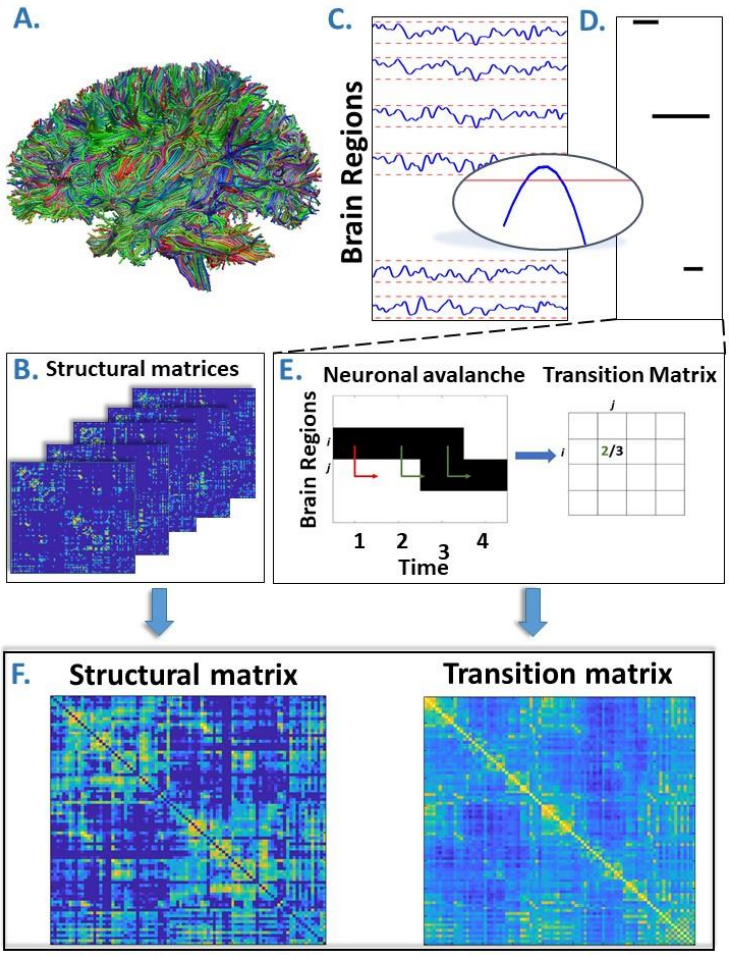

A. Depiction of the human brain tractogram from one subject. **B.** Subject-level structural matrices. Rows and columns represents brain regions, while entries are the number of streamlines connecting any two regions. **C.** Source-reconstructed MEG series. Each blue line represents the z-scored activity of a region, and the red lines denote the threshold (z-score= ± 3). The inlet represent a magnified version of a time-series exceeding the threshold. **D.** Raster plot of an avalanche. For each region, the moments in time when the activity is above threshold are represented in black, while the other moments are indicated in white. The particular avalanche that is represented involved three regions. **E.** Estimation of the transition matrix of a toy avalanche. Regions *i* is active three times during the avalanche. In two instances, denoted by the green arrows, region *j* has been active after region *i*. In one instance, denoted by the red arrow, region *i* is active but region *j* does not activate at the following time step. This situation would result, in the transition matrix, as a 2/3 probability. **F.** Average structural matrix and average transition matrix (Log scale).

Figure 2.

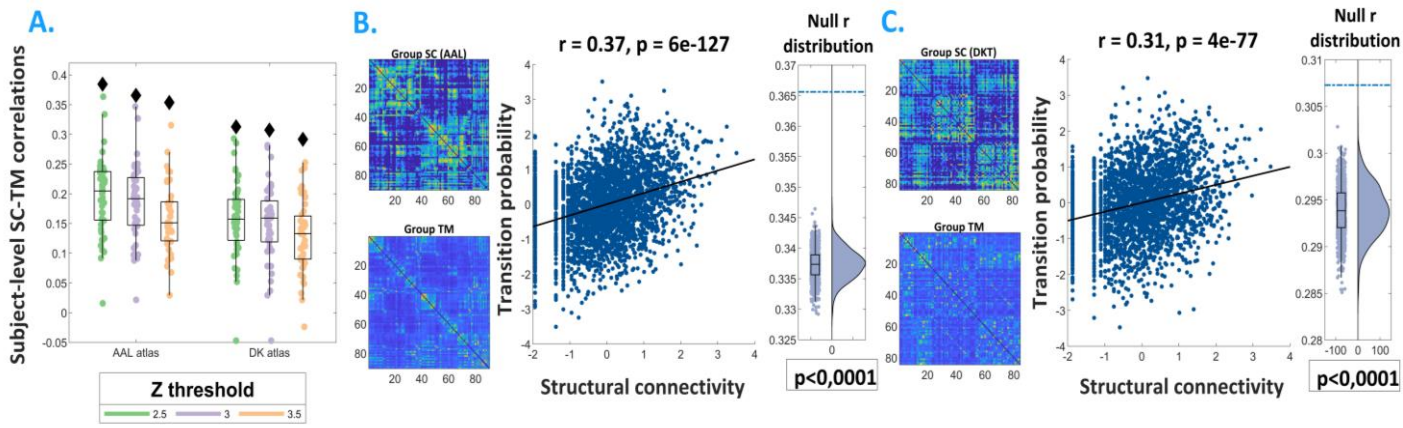

A. Distribution of the r's of the Spearman's correlation between the subject-specific transition matrices and structural connectomes. The black diamond represent the r's of the group-averaged matrices. On the left, the results for the AAL atlas, on the right, the results for the DKT atlas. Green, purple and orange dots represent results obtained with a z-score threshold of 2.5, 3 and 3.5, respectively. **B and C.** Data referring to the AAL atlas in B, to the DKT atlas in **C.** On the top-left, the average structural matrix, on the bottom left, the average transition matrix. The scatterplot shows the correlation between the values of the structural edges and the transition probabilities for the corresponding edge. The black line represents the best fit line in the least-square sense. On the right, the distribution shows the r's derived from the null distribution. The dotted blue line represents the observed r.